THE JOURNAL OF PHYSICAL CHEMISTRY B

Article

pubs.acs.org/JPCB

Self-Ordering Properties of Functionalized Acenes for Annealing-Free Organic Thin Film Transistors

Paul Bazylewski,[†] Kyung Hwan Kim,[‡] Dong Hoon Choi,[‡] and Gap Soo Chang*[,†]

[†]Department of Physics and Engineering Physics, University of Saskatchewan, Saskatoon, Saskatchewan, S7N 5E2, Canada

[‡]Department of Chemistry, Research Institute for Natural Sciences, Korea University, Seoul 136-713, South Korea

Supporting Information

ABSTRACT: Presented here is a study of the molecular self-ordering properties of four bis(phenylethynyl) anthracene based organic semiconductors related to their electronic structure employing X-ray spectroscopy techniques and density functional theory (DFT) calculations. The local molecular order through polarization dependence of C 1*s* → π^* transitions revealed ordered π-stacking nearly perpendicular to the substrate due to van der Waals interactions between alkyl groups. DFT calculations were used to deconvolute the measured electronic structure and examine effects of small changes in molecular geometry in relation to measured charge carrier mobility in top contact field effect transistors. The highest occupied molecular orbital (HOMO) and lowest unoccupied molecular orbital (LUMO) are found to be conjugated from the anthracene core across the bridging ethynyl groups to the thiophene and phenyl end groups. The inclusion of ethynyl bridges connecting the thiophenes has a twofold effect of both reducing the rotational freedom of this functional group and increasing HOMO/LUMO conjugation across the molecules. These features help create a more rigid upright structure for HB-ant-THT with better molecular orbital conjugation and subsequent higher mobility. With this understanding of how different functional groups interact with an acene core, future synthesis of new materials may be directed toward annealing-free organic semiconducting materials.

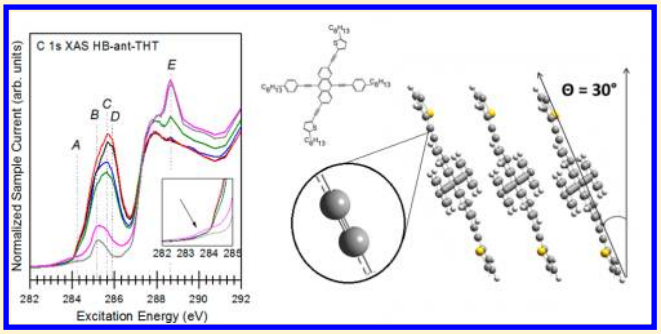

INTRODUCTION

Recently, there has been great progress in the development of organic semiconductor materials for electronics applications. The *p*-type organic semiconductors such as pentacene, rubrene, and thiophene containing polymers have been used to produce organic thin-film transistors (OTFTs) showing carrier mobilities of up to about 1 $cm^2/V{\cdot}s$.[1−3] However, the achievement of this performance often requires complex fabrication procedures involving vapor deposition in vacuum or inert atmosphere, severely limiting their application to low cost, large scale processing. In answer to these difficulties, organic semiconductors soluble in common organic solvents have been developed for solution processing techniques. Although this method is better suited to large scales, the quality of the produced films is typically inferior, often displaying disordered molecular arrangements. Amorphous phase or highly dense grain boundaries is the primary reason for poor electrical properties[4] and thus requires a post-treatment process such as annealing in order to improve crystallinity and film uniformity. The requirement of postannealing to temperatures of >100 °C also limits the choice of substrate, preventing the use of common flexible substrates such as poly(ethyleneterephthalate) (PET). Annealing is therefore another major challenge for cost-effective large-scale production of organic electronics devices.

Due to these difficulties, much work has focused on design of new materials which intrinsically possess a desirable propensity to crystallize into ordered structure. A donor−acceptor polymer semiconductor based on diketopyrrolopyrrole (DPP) and β-unsubstituted quaterthiophene (QT) has been recently synthesized displaying a remarkably high hole mobility of 0.89 $cm^2/V{\cdot}s$ forming a layered lamellar structure with $\pi-\pi$ stacking parallel to the substrate without thermal annealing.[5] On the other hand, acene derivatives with pentacene and anthracene core units have also been investigated in an effort to develop the soluble small-molecule semiconductors, such as bis(triisopropylsilylethynyl) (TIPS)-pentacene. Despite these effort, they display generally low carrier mobility (<0.1 $cm^2/V{\cdot}s$),[6−8] and in the case of TIPS-pentacene the bulky side groups also result in high variability in crystallization, with similarly prepared films often displaying greatly varying structural motifs.[9]

In the present work, we investigate the self-ordering properties of a class of bis(phenylethynyl)anthracene (BPEA)-based semiconductor materials (hereafter referred to as B-ant-HT, B-ant-THT, HB-ant-HT, and HB-ant-THT)

Received: June 12, 2013
Revised: August 13, 2013
Published: August 14, 2013

 © 2013 American Chemical Society

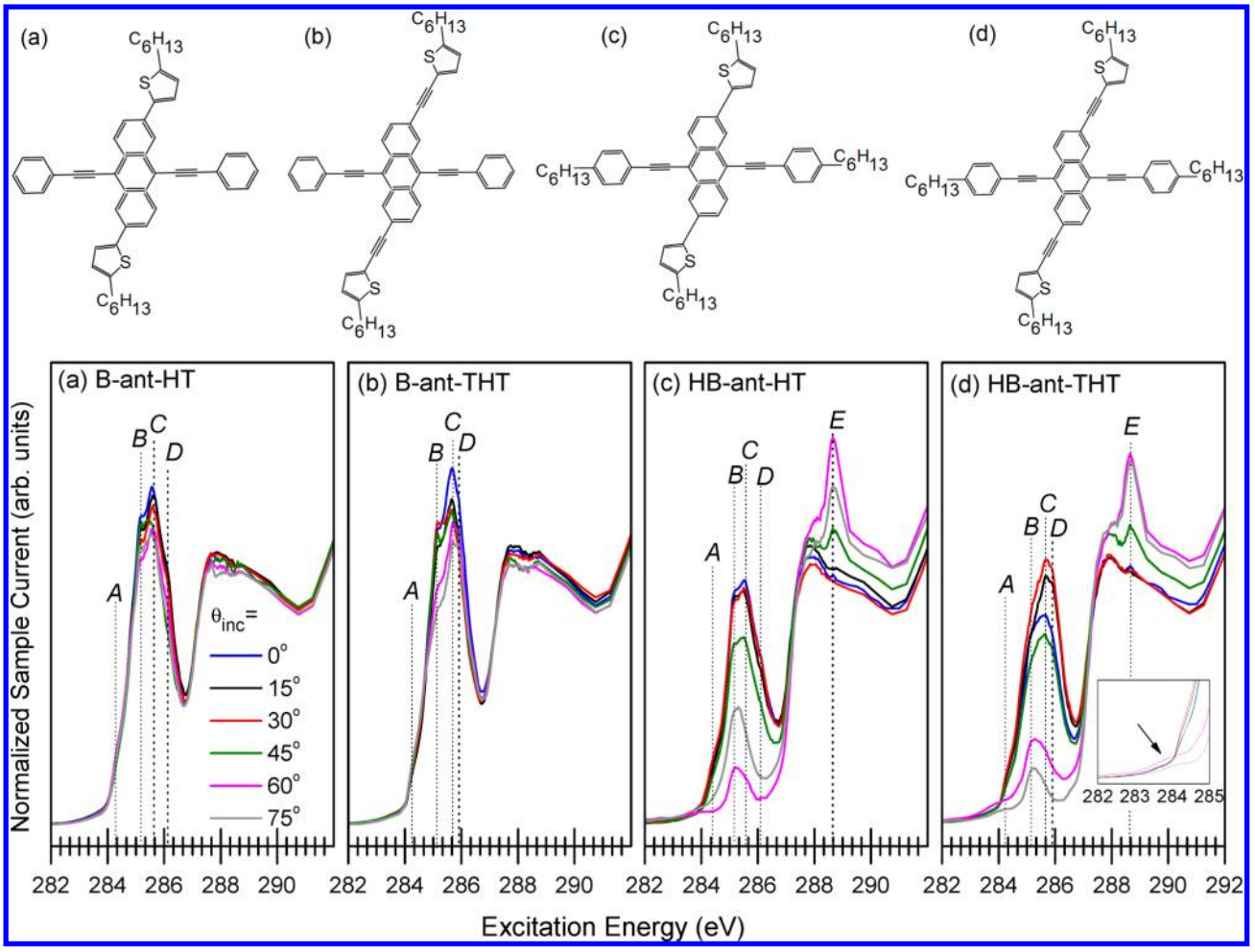

Figure 1. Angle-resolved C 1*s* NEXAFS spectra in TEY mode for (a) B-ant-HT, (b) B-ant-THT, (c) HB-ant-HT, and (d) HB-ant-THT thin films where θ_{inc} is the incidence angle of X-rays on the sample relative to the surface normal. Clear evidence of local structure is observed through polarization dependence in HB-ant-HT and HB-ant-THT. A close view of the edge onset is shown in the inset of (d), indicating resonances visible at grazing incidence.

which display a highly ordered structure in solution-processed films without additional annealing.[10,11] As a short note on the naming convention used, these molecules are given short names where the prefix "HB" indicates alkyl side groups, "B" simply a phenyl, and the suffix "THT" refers to an ethynyl bridge between the thiophene and anthracene, with "HT" being a simple single bond.

OTFTs based on spin-cast films of these materials have shown the charge carrier mobility of 0.24 $cm^2/V{\cdot}s$ and up to 0.40 $cm^2/V{\cdot}s$ in single crystals grown from tetrahydrofuran (THF) solution.[10,12] This mobility is relatively large for OTFTs where carrier mobility rarely approaches 0.1 $cm^2/V{\cdot}s$ in devices constructed without a postannealing step.[6−8] These BPEA-based X-shaped materials are very similar structurally, differing by only the addition of alkyl chains and ethynyl groups, but display nontrivial variation in electrical and structural characteristics. This study seeks to elucidate the origin of self-ordering arrangement in these materials, as well as characterize the molecular orbital structure in the context of the minor structural differences they present. The electronic properties and molecular-stacking structure have been investigated employing synchrotron-radiation X-ray spectroscopy techniques and density functional theory (DFT) calculations. Angle-resolved near-edge X-ray absorption fine structure (NEXAFS) spectroscopy performed on thin films fabricated without a postannealing show a clear polarization dependence in π^* features for HB-ant-HT and HB-ant-THT, suggesting molecular self-order. The other two materials (B-ant-HT and B-ant-THT) are by contrast determined to be nearly amorphous. The ordering is due to additional alkyl chains not present for B-ant-HT and B-ant-THT which promote the ordering through van der Waals intermolecular interaction. The DFT calculations are used to examine the electronic structure and show that the highest occupied molecular orbital (HOMO) extends across the ethynyl bridges to the thiophene and phenyl end groups when they are in a coplanar arrangement with the anthracene core. The ethynyl attachment of the thiophene is also found to reduce the rotational freedom of this group and modify the molecular orbital distribution of the anthracene core.

■ EXPERIMENTAL METHODS

For spectroscopic measurements, powder samples of the four semiconductors were synthesized in the Department of Chemistry at Korea University, South Korea. Details of materials synthesis can be found in ref 11. Spin-coated films were fabricated on $SiO_2(100)$ substrates using 1 mL of 10% solution by weight with chloroform solvent. The samples were spun at 1000 rpm for 30 s and allowed to dry in atmosphere.

dx.doi.org/10.1021/jp405828d | *J. Phys. Chem. B* 2013, 117, 10658−10664

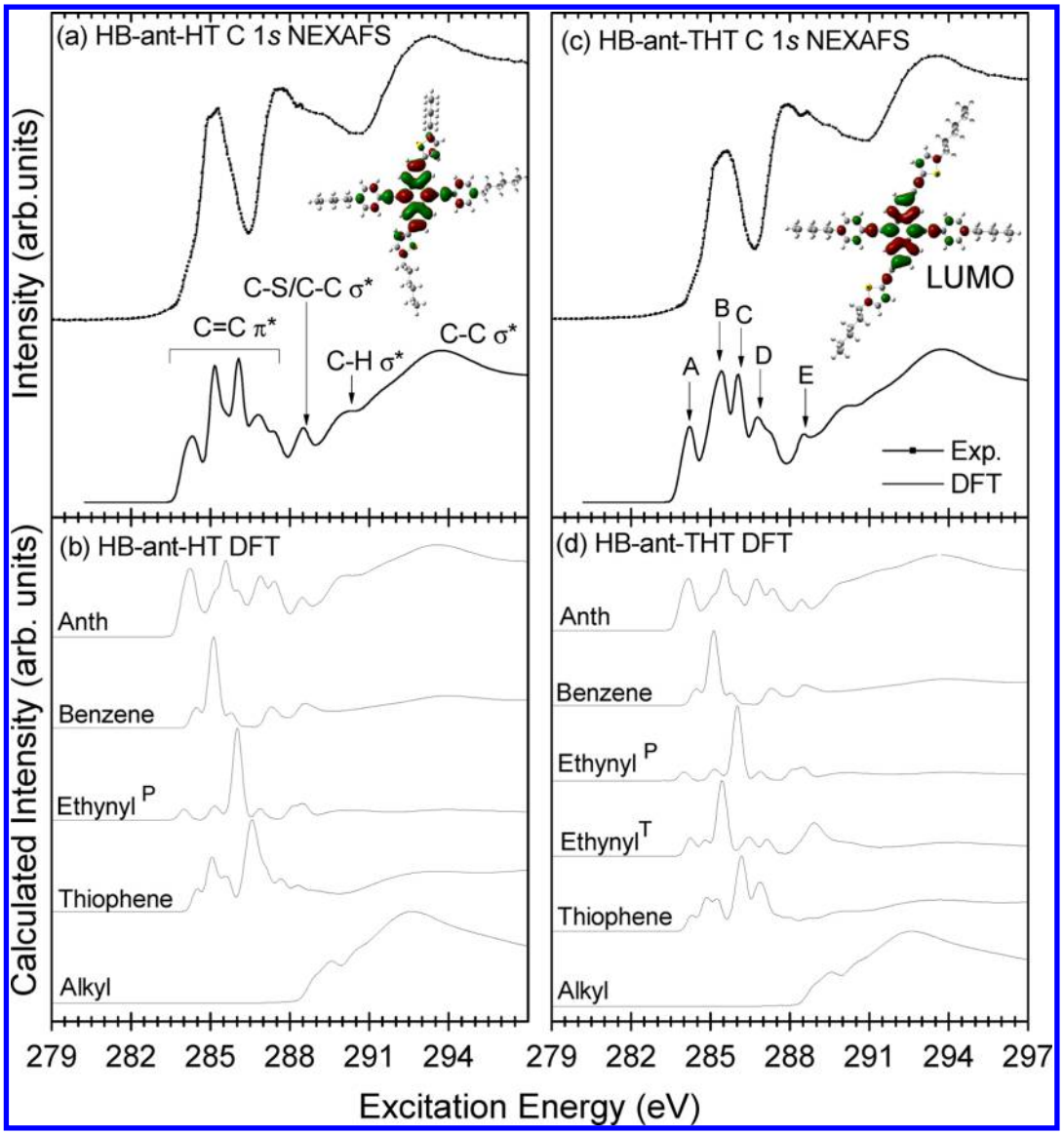

Figure 2. Comparison of (a) HB-ant-HT and (c) HB-ant-THT NEXAFS (top panels) with DFT simulations (b–d). In the top panels, the LUMO isosurfaces for these molecules are shown calculated with GAUSSIAN03. The bottom panel shows the contribution to calculated spectrum from each molecular constituent, identifying the origin of the spectral peaks marked in Figure 1.

Carbon 1*s* NEXAFS measurements in total electron yield (TEY) mode were performed at the Spherical Grating Monochromator (SGM) beamline at the Canadian Light Source (CLS) of the University of Saskatchewan. Carbon Kα X-ray emission spectra (XES) were measured at Beamline 8.0.1 of the Advanced Light Source (ALS) in Berkeley, CA. The energy calibration was performed with the π^* (C═C) transition at 285.4 eV of highly ordered pyrolytic graphite (HOPG) reference sample. The BPEA thin films were tested for radiation damage due to the sensitivity of organic materials to X-ray radiation by five repeated absorption measurements of the near-edge region of 50 s duration on the same sample spot. The spectra showed minimal change in the intensity of spectral features, but no changes in energy position or number of peaks was observed. As a precaution, the sample measurements were taken with the beam spot at different sample locations to minimize the X-ray exposure as much as possible. The measured NEXAFS spectra were normalized to the incoming photon flux by dividing each spectrum by the incident beam intensity (I_0) as recorded by a photodiode. This method was used to correct for spectral artifacts that can appear due to contamination of the Au mesh typically used to measure I_0.

The DFT calculations were performed using the StoBe (Stockholm-Berlin) package which implements Kohn–Sham DFT.[13] The oscillator strengths for core-level excitations to unoccupied states were computed for each atom individually, and summed to produce the total spectrum. The oscillator strengths describing the transition from the core level to the unoccupied molecular orbitals were computed using the transition-state approximation where a half occupied core hole is used and all unoccupied states are left empty. For comparison with measurements, simulated spectra were broadened by convolution with Gaussian functions with full width at half-maximum (fwhm) of 0.4 eV up to 290 eV, and then linearly increasing up to 4.5 eV over the next 10 eV. This broadening scheme uses narrower functions to better model near-edge features which have typical widths of 0.2–0.5 eV. Near the ionization potential the width of spectral features

dx.doi.org/10.1021/jp405828d | J. Phys. Chem. B 2013, 117, 10658–10664

increases linearly up to a fwhm of 4−6 eV at higher energies. Including this transitional range in the broadening scheme prevents overlap of near-edge and higher energy broadening functions, and produces a better agreement with the behavior of experimental spectra. Calculations using Gaussian03 were also performed to generate molecular orbital isosurfaces. Nonlocal hybrid Becke three-parameter Lee−Yang−Parr (B3LYP) function with 6-311G basis set was used for both DFT calculations and geometry. Details of the DFT calculations can be found in the Supporting Information.

RESULTS AND DISCUSSION

Figure 1 displays angle-resolved C 1*s* NEXAFS measurements of the four BPEA materials. Of the four, HB-ant-HT and HB-ant-THT show evidence of molecular self-ordering with clear polarization dependence in π^* resonances centered around 285 eV, with the intensity showing a general decrease with increasing angle of incidence. The broad π^* feature is attributed to a convolution of C 1*s* → π^* (C═C) resonances originating from the anthracene, phenyl, ethynyl, and thiophene groups which are all aromatic structures typically possessing unoccupied orbitals in this energy range. The other two materials, B-ant-HT and B-ant-THT, show very slight variations in π^* intensity upon changing the incident angle. This indicates largely amorphous local structure of B-ant-HT and B-ant-THT. It is worth noting that, according to previous X-ray diffraction (XRD) results,[10,11] the structural ordering of these molecules could be improved extrinsically by the octadecyltrichlorosilane (OTS) self-assembled monolayer and postannealing treatments. The HB-ant-HT and HB-ant-THT molecules displaying the polarization dependence possess phenyl-alkyl side groups that promote molecular ordering through interchain interaction. The structural order is precipitated through a balance between alkyl van der Waals and aromatic $\pi-\pi$ interactions while interestingly the thiophene-alkyl groups alone do not. Such an increase in structural order due to alkyl-substitution is not unexpected, and is well-known for P3HT[14] and other alkylated materials such as perylene-diimide derivatives.[15]

To further elucidate the effect of small structural differences on electrical properties between HB-ant-HT and HB-ant-THT, DFT simulations were performed to understand the origin of absorption lines A−E marked in Figure 1. A DFT-simulated NEXAFS spectrum is compared to experimental one and the results are presented in the top panels of Figure 2. The calculated spectrum was computed as the average signal over all possible orientations. The discrepancy in the peak positions in the calculated spectrum is typical of DFT approaches which do not properly model the core hole effect present in the measurements. Nevertheless, the simulations successfully reproduce absorption lines labeled in Figure 1. For HB-ant-HT, peak A (LUMO at 284.35 eV) is contributed from C 1*s* → π^* (C═C) excitations in the anthracene core and ethynyl groups; peak B results from the phenyl, thiophene, and anthracene; peak C from anthracene, ethynyl, and thiophene; peak D from thiophene and anthracene, and peak E from σ^* excitations in the anthracene core. The shoulder just before peak E (288 eV) is due to C 1*s* → σ^* (C−S) excitations commonly seen in thiophene containing materials,[16] and C 1*s* → σ^* (C−C) excitations from the anthracene. The alkyl chains, containing no C═C bonds, do not possess any π^* states and contribute largely to higher energy σ^* states above the ionization potential (IP) at approimately 290 eV. These DFT results were verified by comparison with NEXAFS measurements of anthracene powder (see the Supporting Information), which assigns the LUMO and other main spectral peaks of all molecules to have a large density on the anthracene core. With the LUMO originating from the anthracene and ethynyl, free carriers will be preferentially located on these groups, meaning that charge transport between HB-ant-THT molecules will be more heavily influenced by proximity of the anthracene cores. Therefore, we expect strong variations in electrical properties for small changes in physical film structure.

For HB-ant-THT, peak A (285.25 eV) results again from anthracene and the phenyl-ethynyl combined into a single resonance; peaks B−E follow to same pattern as for HB-ant-HT but with an additional contribution from the thiophene-ethynyl in peak B. Through the use of second derivatives of calculated spectra (see Figure 3), for HB-ant-HT the LUMO is

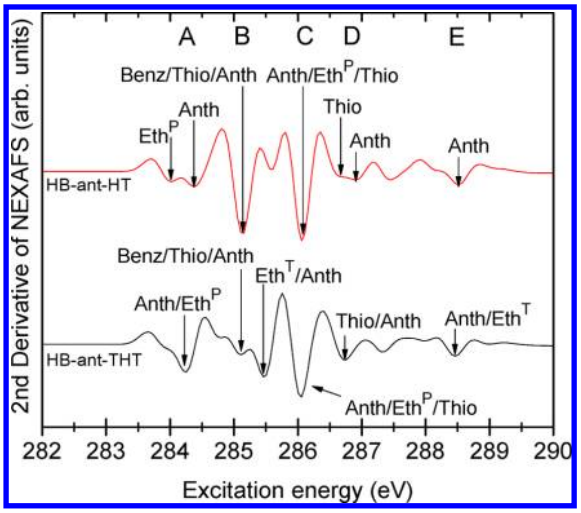

Figure 3. Second derivative curves for the simulated spectra of HB-ant-HT and HB-ant-THT. Peak labels correspond to those in Figure 1 and the labels indicate the molecular origin of each of the π^* resonance features (Eth^P refers to phenyl-anthracene ethynyl; Eth^T to thiophene-anthracene).

separated into two distinct ethynyl and anthracene resonances where they are coincident for HB-ant-THT. Peak B shows the opposite trend where it is a single peak for HB-ant-HT. However, it is a broad combination of two peaks in HB-ant-THT upon addition of the thiophene-ethynyl groups. This broadening is consistent with experimental C 1*s* NEXAFS spectra in Figure 1 where peak B of HB-ant-THT is a broad shoulder (285.1−285.4 eV) as opposed to one of two sharp peaks at 285.1 eV in HB-ant-HT. Given the rigidity of ethynyl groups, it is reasonable to conclude that HB-ant-THT and HB-ant-HT have a planar structure excepting the thiophene of HB-ant-HT. This has been shown to be true for single crystals of HB-ant-THT using XRD.[12] In this configuration, all π^* resonances from aromatic groups will be maximized when excited along the plane of the molecule, excepting the ethynyl attaching the phenyl. This ethynyl will display an intensity maximum at grazing incidence.[17] This is confirmed by a small feature at 284 eV appearing at the grazing incidence (i.e., large θ_{inc}) which arises from π^* excitations in the phenyl-ethynyl [see inset of Figure 1d, bottom]. This feature also appears for HB-ant-HT at grazing incidence while less prominent. The trend of polarization dependence can now be further quantified with the knowledge of molecule's planarity. The HB-an-HT is a mixture of upright structures with tilt angles ranging from 0 to 30°

dx.doi.org/10.1021/jp405828d | J. Phys. Chem. B 2013, 117, 10658−10664

relative to the surface normal as observed by a near constant TEY signal for varying incident angle in this range. HB-ant-THT conversely has an intensity maximum of peak C at 30° with a consistent decrease for increasing angle of incidence. Since peak C is contributed from anthracene-thiophene resonances and HB-ant-THT is rigidly planar due to ethynylation, HB-ant-THT films possess a dominant crystal structure where planar molecules stand upright at 30° relative to the surface normal. Based on the spectroscopic analysis, the model structures of HB-and-THT and HB-ant-HT thin film are present in Figure 4.

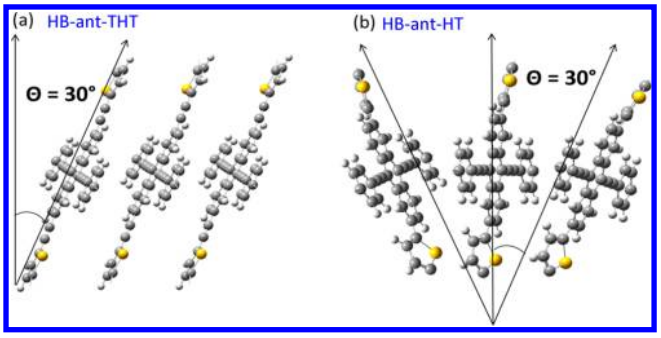

Figure 4. Molecular stacking arrangements for (a) HB-ant-THT with a majority of molecules stacked at 30° relative to the substrate, and (b) HB-ant-HT which has a distribution of stacking angles from 0 to 30° (alkyls removed for clarity).

In addition to angle-resolved C 1*s* NEXAFS, nonresonant XES measurements were conducted to investigate the occupied molecular orbital structure responsible for *p*-type conduction. Figure 5 shows the C Kα XES spectra for B-ant-HT (a) and HB-ant-THT (b) obtained at the excitation energy (E_{exc}) of 320 eV. Of the four molecules examined, B-ant-HT and HB-ant-THT show the least and most molecular ordering, respectively The spectra are fitted with Voigt functions to take account of both the instrumentation and lifetime broadening present in these measurements. Shown in inset of Figure 5 is the HOMO isosurface for these molecules computed with GAUSSIAN03 DFT package. The calculations show little variation between the molecules with the HOMO extending to the phenyl and thiophene groups regardless of the presence of a bridging ethynyl. Peak fitting of the C Kα XES spectra show a variation in the fwhm of the highest energy emission feature representing the HOMO with a larger value for HB-ant-THT. Increased fwhm implies greater delocalization of the HOMO in HB-ant-THT due to alkylation and the subsequent increased molecular ordering. Further fits for B-ant-THT and HB-ant-HT (not shown) reveal fwhm values of 2.68 and 2.54 eV, indicating thiophene-ethynyls improve HOMO delocalization as well as planarity in these molecules.

From previous work, the hole carrier mobility of BPEA-based OTFTs fabricated under ambient conditions without additional annealing is highest for HB-ant-THT (0.24 $cm^2/V{\cdot}s$), followed by B-ant-THT (0.040 $cm^2/V{\cdot}s$), HB-ant-HT (0.014 $cm^2/V{\cdot}s$), and B-ant-HT with the lowest (0.010 $cm^2/V{\cdot}s$).[10,11] This *I*−*V* characteristic is consistent with C Kα XES and C 1*s* NEXAFS where HB-ant-THT possesses the most delocalized HOMO and highly ordered structure. The similar HOMO delocalization due to ethynyl-thiophenes was observed in the XES spectrum of B-ant-THT (not shown). The greater mobility observed for HB-ant-THT is attributed to the $\pi-\pi$ stacking

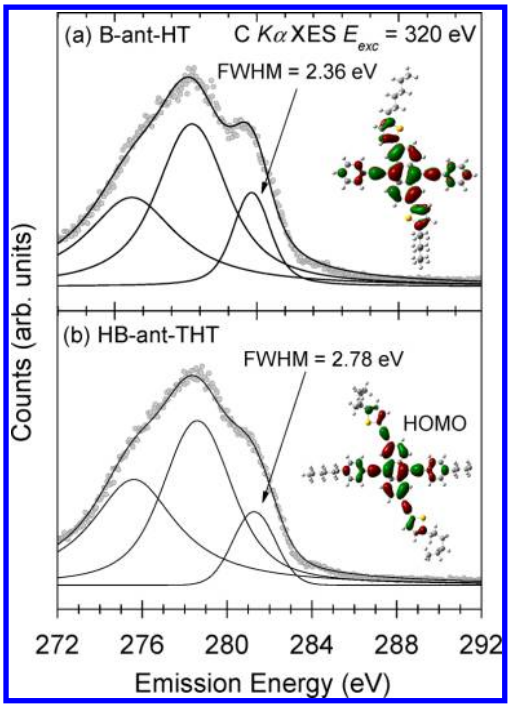

Figure 5. Nonresonant C Kα XES spectra fitted by Voigt functions for (a) B-ant-HT and (b) HB-ant-THT. The corresponding calculated HOMO isosurfaces are shown in the inset. The increase in fwhm is due to greater delocalization of the HOMO across the film for HB-ant-HT. The trend of increasing fwhm and HOMO delocalization is consistent across the set of molecules with B-ant-HT showing the most localized HOMO.

induced by alkylation and molecular rigidity imposed by the ethynyl-thiophene groups.

Of the four materials, HB-ant-HT displays the lowest hole mobility in spite of its ordered local structure and greater HOMO delocalization than B-ant-HT. For comparison, NEXAFS analysis shows the self-order of HB-ant-THT is determined to have a dominant phase of molecules stacked upright at 30° relative to the surface normal as shown in Figure 4. The HOMO overlap between neighboring molecules will be increased provided that molecules stack face-to-face, and account for high carrier mobility. The HB-ant-HT also takes an average upright structure, but in a mixture of structural configurations (see Figure 5). The mixture is accounted for by considering the rotational freedom of the thiophene groups which lack rigid ethynyl bridges, allowing the thiophenes to freely rotate and produce a less uniform structure compared to HB-ant-THT. Structural order in HB-ant-HT may be limited by dispersion forces such as dipole−dipole, hydrogen bonding, and C−H/π bonding. Such forces are known to contribute strongly to the film forming properties of aromatic materials with planar ligands.[18,19] C−H/π bonding in particular could contribute where the C−H bond has been shown to preferentially point toward the plane of an aromatic ring.[20] With the thiophene free to rotate, C−H/π interactions may form between the thiophene and alkyl chains of neighboring molecules, reducing molecule planarity. DFT calculations that take into account such dispersion forces (DFT-D) have been performed for more complex systems such as guanine aggregates[18] and bis-dithiazolyl radicals.[19] These results show specific contributions from dipole−dipole and C−H/π interactions that give rise to a large number of possible

dx.doi.org/10.1021/jp405828d | J. Phys. Chem. B 2013, 117, 10658−10664

molecular arrangements. It is reasonable to conclude that such forces act in a similar fashion in the present system producing structural variations in HB-ant-HT. Future attempts to further understand these materials should utilize dispersion basis sets to better model film structure in materials such as HB-ant-HT.

Concerning the mobility difference between HB-ant-THT and HB-ant-HT in the hopping transport regime, considering the reorganization energy and overlap integrals can help explain the discrepancy. For the case of a hopping process, Marcus theory may be utilized in a similar fashion to ref 21 to calculate the rate of charge transfer, W, between two neighboring molecules. This charge transfer rate is then proportional to charge carrier mobility through a diffusion coefficient.[21] W can be expressed as shown in eq 1 and is proportional to the coupling matrix element H_{mn} between two nighbouring molecules (m,n) and inversely proportional to the reorganization energy λ (where T is temperature and k_B the Boltzmann constant).

$$W = \frac{2{H_{mn}}^2}{h}\left(\frac{\pi^3}{\lambda k_B T}\right)^{1/2} \exp\left(\frac{\lambda}{-4k_B T}\right) \quad (1)$$

Charge carrier mobility is maximum for HB-ant-THT, suggesting that W is also large for this molecule, corresponding to a minimal λ and large H_{mn}. Reorganization energy contains two parts; internal reorganization energy being the energy required for molecular structure changes when an electron is added or removed from the molecule, and the external reorganization energy which is due to structural modifications that occur in the surrounding medium due to the electron transfer process.[22] HB-ant-THT possesses a rigid planar structure that is more resistant to structural changes during charge transfer, resulting in similar neutral ground state and excited state geometries, and subsequent lower internal reorganization energy. According to HOMO and LUMO isosurface calculations, charge transfer will also occur primarily between anthracene cores which are the most rigid part of the molecule and therefore relatively insensitive to reorganization. HB-ant-HT in contrast possesses more structural freedom and may undergo significant reorganization in the thiophene end groups during charge transfer, leading to larger λ. The charge transfer matrix elements can also be examined in the Marcus−Hush two state model assuming a dimer configuration and four possible states resulting from the dimer configuration for of two molecules m and n, namely, the LUMO, LUMO + 1, HOMO, HOMO − 1.[21] H_{mn} for hole transport is proportional the difference between the HOMO and HOMO − 1 levels in such a configuration. Although these calculations have not been performed here, examining the XES results (Figure 5) shows HB-ant-THT and HB-ant-HT to have very similar occupied states and no significant energy shift in the HOMO between molecules. H_{mn} is therefore similar between these two molecules and indeed between all four studied in this work. In the framework of Marcus−Hush theory, W is therefore maximal for HB-ant-THT with a smaller reorganization energy, which when combined with an ordered stacking structure results in large charge carrier mobility. HB-ant-HT shows reduced structural order due to dispersion forces which produce a variety of molecular orientations. This coupled with larger reorganization energy due to the rotational freedom of the thiophene group results in overall lower charge carrier mobility for HB-ant-HT.

CONCLUSIONS

The self-ordering properties in the bis(phenylethynyl) anthracene-based organic semiconductors has been investigated employing soft X-ray spectroscopy. The C1s NEXAFS results clearly showed the ordered structure in the molecules with alkyl side groups, with a polarization dependence and indicated that the molecules are π-stacked parallel to the substrate. The molecular orbital structure of both occupied and unoccupied states has been further analyzed using the combination of NEXAFS, XES, and DFT calculations. It is evident that molecules with an anthracene core and thiophene functional groups provide a well conjugated HOMO ideal for p-type conduction. The addition of alkyl chains to all functional groups has been shown to produce an ordered structure, but the nature and uniformity of the stacking may also be greatly influenced by the other functional groups. In this case, the rotational freedom of the thiophenes in HB-ant-HT when no ethynyl is present results in a mixture of crystal structures that is detrimental to the carrier mobility. HB-ant-THT is determined to have the highest performance due to alkylation and a rigid planar structure, and takes an average orientation standing upright at 30° relative to the substrate normal. HB-ant-HT is in contrast limited by a lack of stabilizing ethynyl groups causing structural variations and larger reorganization energy, resulting in mobility an order of magnitude lower than that of HB-ant-THT. Therefore, if new acene-based materials are to be designed, they require alkylated aromatic functional groups that are rigidly held in a planar geometry. Ethynyl groups were found to impart rigidity and support the molecular orbital conjugation, ideal for this application. With this knowledge, work may be continued with related structures to produce a family of acene-based materials displaying highly crystalline structures without the need for postannealing treatment.

ASSOCIATED CONTENT

Supporting Information

Detailed discussion of the method used for electronic structure calculations using both StoBe and GAUSSIAN03. Peripheral X-ray absorption measurements used to assign spectral features (Figure S2) and detailed calculation results used to construct Figure 3 (see Table S1). This material is available free of charge via the Internet at http://pubs.acs.org.

AUTHOR INFORMATION

Corresponding Author

*Telephone: 306-966-2768. Fax: 306-966-6400. E-mail: gapsoo.chang@usask.ca.

Notes

The authors declare no competing financial interest.

ACKNOWLEDGMENTS

We gratefully acknowledge support from the Natural Sciences and Engineering Research Council of Canada (NSERC) and Canada Foundation for Innovation (CFI). D.H.C. is thankful for the support from the National Research Foundation of Korea (NRF2012R1A2A1A01008797) and by Key Research Institute Program (NRF20120005860). Canadian Light Source is supported by the Natural Sciences and Engineering Research Council of Canada, the National Research Council Canada, the Canadian Institutes of Health Research, the Province of Saskatchewan, Western Economic Diversification Canada, and

the University of Saskatchewan. The Advanced Light Source is supported by the Director, Office of Science, Office of Basic Energy Sciences, of the U.S. Department of Energy under Contract No. DE-AC02-05CH11231.

REFERENCES

(1) Meng, Q.; Dong, H.; Hu, W.; Zhu, D. Recent Progress of High Performance Organic Thin Film Field-Effect Transistors. *J. Mater. Chem.* **2011**, *21*, 11708−11721.
(2) Tsao, H. N.; Cho, D. M.; Park, I.; Hansen, M. R.; Mavrinskiy, A.; Yoon, D. Y.; Graf, R.; Pisula, W.; Spiess, H. W.; Müllen, K. Ultrahigh Mobility in Polymer Field-Effect Transistors by Design. *J. Am. Chem. Soc.* **2011**, *133*, 2605−2612.
(3) Li, Y.; Singh, S. P.; Sonar, P. A High Mobility P-Type DPP-Thieno[3,2-b]thiophene Copolymer for Organic Thin-Film Transistors. *Adv. Mater.* **2010**, *22*, 4862−4866.
(4) Dimitrakopoulos, C. D.; Malenfant, P. R. L. Organic Thin Film Transistors for Large Area Electronics. *Adv. Mater.* **2002**, *14*, 99−117.
(5) Li, Y.; Sonar, P.; Singh, S. P.; Soh, M. S.; van Meurs, M.; Tan, J. Annealing-Free High-Mobility Diketopyrrolopyrrole-Quaterthiophene Copolymer for Solution-Processed Organic Thin Film Transistors. *J. Am. Chem. Soc.* **2011**, *133*, 2198−2204.
(6) Schmidt, R.; Göttling, S.; Leusser, D.; Stalke, D.; Krause, A. M.; Würthner, F. Highly soluble acenes as semiconductors for thin film transistors. *J. Mater. Chem.* **2006**, *16*, 3708−3714.
(7) Park, J.-H.; Chung, D. S.; Park, J.-W.; Ahn, T.; Kong, H.; Jung, Y. K.; Lee, J.; Yi, M. H.; Park, C. E.; Kwon, S.-K.; Shim, H.-K. Soluble and Easily Crystallized Anthracene Derivatives: Precursors of Solution-Processable Semiconducting Molecules. *Org. Lett.* **2007**, *9*, 2573−2576.
(8) Cui, W.; Zhang, X.; Jiang, X.; Tian, H.; Yan, D.; Geng, Y.; Wang, F. Synthesis and Characterization of Soluble Oligo (9,10-Bisalkynylanthrylene)s. *Org. Lett.* **2006**, *8*, 785−788.
(9) He, Z.; Xiao, K.; Durant, W.; Hensley, D. K.; Anthony, J. E.; Hong, K.; Kilbey, S. M., II; Chen, J.; Li, D. Enhanced Performance Consistency in Nanoparticle/TIPS Pentacene-Based Organic Thin Film Transistors. *Adv. Funct. Mater.* **2011**, *21*, 3617−3623.
(10) Jung, K. H.; Bae, S. Y.; Kim, K. H.; Cho, M. J.; Lee, K.; Kim, Z. H.; Choi, D. H.; Lee, D. H.; Chung, D. S.; Park, C. E. High-mobility anthracene-based X-shaped conjugated molecules for thin film transistors. *Chem. Commun.* **2009**, *35*, 5290−5292.
(11) Bae, S. Y.; Jung, K. H.; Hoang, M. H.; Kim, K. H.; Lee, T. W.; Cho, M. J.; Jin, J.-I.; Lee, D. H.; Chung, D. S.; Park, C. E.; Choi, D. H. 9,10-Bis(phenylethynyl)anthracene-based organic semiconducting molecules for annealing-free thin film transistors. *Synth. Met.* **2010**, *160*, 1022−1029.
(12) Kim, K. H.; Bae, S. Y.; Kim, Y. S.; Hur, J. A.; Hoang, M. H.; Lee, T. W.; Cho, M. J.; Kim, Y.; Kim, M.; Jin, J.-I.; Kim, S.-J.; Lee, K.; Lee, S. J.; Choi, D. H. Highly Photosensitive J-Aggregated Single-Crystalline Organic Transistors. *Adv. Mater.* **2011**, *23*, 3095−3099.
(13) Hermann, K.; Pettersson, L. G. M.; Casida, M. E.; Daul, C.; Goursot, A.; Koester, A.;Proynov, E.; St-Amant, A.; Salahub, D. R. Contributing authors: Carravetta, V.; Duarte, H.; Friedrich, C.; Godbout, N.; Guan, J.; Jamorski, C.; Leboeuf, M.; Leetmaa, M.; Nyberg, M.; Patchkovskii, S.; Pedocchi, L.; Sim, F.; Triguero, L.; Vela, A. *StoBe-deMon*, version 3.0, 2009.
(14) Prosa, T. J.; Winokur, M. J.; Moulton, J.; Smith, P.; Heeger, A. J. X-ray structural studies of poly(3-alkylthiophenes): an example of an inverse comb. *Macromolecules* **1992**, *25*, 4364−4372.
(15) Kamm, V.; Battagliarin, G.; Howard, I. A.; Pisula, W.; Mavrinskiy, A.; Li, C.; Müllen, K.; Laquai, F. Polythiophene:Perylene Diimide Solar Cells − the Impact of Alkyl-Substitution on the Photovoltaic Performance. *Adv. Energy Mater.* **2011**, *1*, 297−302.
(16) Salleo, A.; Kline, R. J.; DeLongchamp, D. M.; Chabinyc, M. L. Microstructural Characterization and Charge Transport in Thin Films of Conjugated Polymers. *Adv. Mater.* **2010**, *22*, 3812−3838.
(17) Stöhr, J. *NEXAFS Spectroscopy*; Springer-Verlag: Berlin, 1996.
(18) Jissy, A. K.; Datta, A. Effect of External Electric Field on H-Bonding and π-Stacking Interactions in Guanine Aggregates. *ChemPhysChem* **2012**, *13*, 4163−4172.
(19) Jose, D.; Datta, A. Role of Multicentered Bonding in Controlling Magnetic Interactions in π-Stacked Bis-dithiazolyl Radical. *Cryst. Growth Des.* **2011**, *11*, 3137−3140.
(20) Tsuzuki, S.; Fujii, A. Nature and physical origin of CH/π interaction: significant difference from conventional hydrogen bonds. *Phys. Chem. Chem. Phys.* **2008**, *10*, 2584−2594.
(21) Datta, A.; Mohakud, S.; Pati, S. K. Electron and hole mobilities in polymorphs of benzene and naphthalene: Role of intermolecular interactions. *J. Chem. Phys.* **2007**, *126*, 144710.
(22) Jose, D.; Datta, A. Structures and electronic properties of silicene clusters: a promising material for FET and hydrogen storage. *Phys. Chem. Chem. Phys.* **2011**, *13*, 7304−7311.